Circulation Induced by River Inflow in Well Mixed Water over a Sloping Continental Shelf[1]

G. T. CSANADY

Woods Hole Oceanographic Institution, Woods Hole, MA 02543

(Manuscript received 23 January 1984, in final form 13 August 1984)

ABSTRACT

The pressure field over a sloping continental shelf subject to freshwater runoff at the coast can be resolved into a nearly two-dimensional dynamic height field and a residual field, the latter arising from the interaction of baroclinity and topography. The residual field is essentially three-dimensional and so constituted as to supply the fluid for the baroclinic alongshore flow off a coastal source of buoyancy associated with the cross-isobath density gradients. The intensity of the induced residual circulation (its total transport in m^3 s^{-1}) varies directly with the buoyancy input and bottom slope, and inversely with the zero-order alongshore flow velocity and Coriolis parameter. Over the Mid-Atlantic Bight continental shelf the runoff-induced residual circulation makes a generally weak contribution to the observed mean flow field. It could, however, be more important over a low-latitude shelf subject to high runoff.

1. Introduction

Simple dynamical arguments show that variations of density over a sloping seafloor, along lines of constant depth, tend to generate a depth-independent pressure field, i.e., a pattern of horizontal circulation. With idealizations appropriate to continental shelf dynamics, the effect shows up as a source term in the vorticity-tendency equation, containing along-isobath density gradients (Hsueh *et al.*, 1976; Hendershott and Rizzoli, 1976; Csanady, 1979). The calculation of the resulting flow field is made difficult usually by the nonlinear interaction of the flow and density fields, manifesting itself in a self-advection of the density distribution by its own induced flow field. Previous studies of the phenomenon have therefore been numerical (Hendershott and Rizzoli, 1976) or confined to specific aspects of flow development (Shaw, 1982; Shaw and Csanady, 1983).

The complications introduced by advection are irrelevant to the general problem of baroclinity–topography interaction and it should be possible to neglect them in a first approximation in a suitably linearized model. One is naturally led to such a model by considering the circulation induced by low-intensity freshwater sources on a continental shelf, over a long stretch of coastline.

Freshwater runoff from land affects the density field over continental shelves and generates a pattern of thermohaline circulation. The simplest models of runoff-driven circulation are two-dimensional and ignore depth variations (Stommel and Leetmaa, 1972; Kao, 1981). Something like a Hadley cell arises in the cross-shore plane, driving baroclinic flow parallel to the coast, along lines of constant density. Observations show the most intense currents in this type of flow to occur along a surface-to-bottom front separating fresher coastal waters from more saline waters offshore (Beardsley and Flagg, 1976; Blanton and Atkinson, 1983; Royer, 1981). In the Mid-Atlantic Bight such a front can be observed at the edge of the shelf in winter, when winds and surface cooling combine to maintain a vertically nearly homogeneous water mass shoreward of the front. The location and characteristics of this front are of great current interest, but are not further considered here.

Although the shore-side water mass is nearly homogeneous in winter, river plumes are nevertheless discernible in it, e.g., off the Hudson estuary or Chesapeake Bay (Bowman and Wunderlich, 1977; Boicourt, 1982). The water column is nearly well mixed vertically, but is subject to along-isobath density changes, which may conceivably induce circulation of local importance, or affect through their aggregate influence far downstream portions of the shelf. Because the density changes involved are small (much smaller than those across the principal density front at the edge of the shelf) one expects the river plume-induced circulation to be a small perturbation on a more vigorous large-scale pattern impressed by winds and by deep ocean effects. The self-advection of the density field may then be ignored, and a linearized, diagnostic model constructed of the induced circulation.

[1] Woods Hole Oceanographic Institution Contribution Number 5603.

While the idealizations made in the present approach are drastic, they are complementary to those made in the two-dimensional models. The results reveal certain three-dimensional effects not even hinted at by two-dimensional models and illustrate in a concrete manner the pattern of circulation attributable to the vorticity-generating effect of along-isobath density variations. The theory also supplies simple quantitative relationships, exhibiting the relative importance of the various physical factors governing the baroclinity–topography interaction, the value of which to some extent transcends the idealizations of the specific model adopted.

The principal assumptions of the model are as follows; see Fig. 1 for schematic illustration. The density field is maintained by the diffusion of freshwater from a finite-length distributed coastal source into a wedge of fluid of small angle (≡ bottom slope s). The zero-order alongshore velocity v_0 is constant and large compared to perturbation velocities. Horizontal diffusion is due to current shear and hence very effective; see e.g., the discussion by Csanady (1982, p. 226). It is parameterized by a large effective diffusivity K. Vertically, the water column is supposed well mixed. The alongshore scale (length of the source region) is taken to be long enough for advection to dominate diffusion in the alongshore direction ($vY/K \gg 1$). The density of the fluid is related to freshwater concentration through an equation of state describing the empirical mixing line in the T–S diagram between shelfwater and slopewater. The boundary condition at infinity is zero freshwater concentration: the presence of a distant edge-of-the-shelf front is ignored and only coastally trapped density and flow fields are considered.

The circulation generated by the density field calculated according to the above assumptions is supposed steady and subject to linearized equations of motion with linear bottom friction. As in other related problems (Csanady 1978, 1979) the relevant cross-isobath length scale is:

$$L = \left(\frac{rY}{fs}\right)^{1/2},$$

where r is a bottom resistance coefficient and f the Coriolis parameter. At midlatitudes, L is typically 10 km or more. Thus the Rossby number v/fL formed with the zero-order advection velocity is small, as is the ratio of horizontal to vertical friction force. The equation for the induced pressure field is then as used in earlier studies of this kind (Csanady, 1979; Shaw and Csanady, 1983), and simple heat conduction-type solutions are readily found. Viewed as an extension of those earlier studies, the present paper gives concrete examples of circulation induced by realistic along-isobath variations of bottom density, arrived at analytically.

2. Freshwater diffusion

The coordinate system used is shown in Fig. 1. Given the idealizations just described, the concentration of freshwater χ in the wedge between the surface and the bottom is subject to the equation:

$$v_0 sx \frac{\partial \chi}{\partial y} = \frac{\partial}{\partial x}\left(Ksx \frac{\partial \chi}{\partial x}\right) + \frac{\partial}{\partial y}\left(Ksx \frac{\partial \chi}{\partial y}\right). \quad (1)$$

The boundary condition at the coast is constant inflow rate over a limited segment of the coast:

$$\left.\begin{aligned} q = -Ksx \frac{\partial \chi}{\partial x}\bigg|_{x=0} &= \text{constant}, \quad y_1 < y < y_1 + Y \\ q &= 0, \quad \text{otherwise} \end{aligned}\right\}. \quad (2)$$

Far from the coast the concentration of freshwater is negligible:

$$\chi = 0, \quad x \to \infty. \quad (3)$$

The advection number A of the problem (akin to Peclét number) is supposed large:

$$A = \frac{vY}{K} \gg 1, \quad (4)$$

so that alongshore advection dominates diffusion. Typical quantities to be used in estimates below are $v_0 = 0.1$ m s^{-1}, $K = 300$ m^2 s^{-1}, $Y = 5 \times 10^5$ m, giving $A = 165$. The second term on the right of Eq. (1) may then be dropped. The value of K is consistent with shear diffusion and comparable to empirically deduced values of Ketchum and Keen (1955) and Loder *et al.* (1982).

The remaining simple parabolic equation contains the time-like coordinate y/v_0. For a source at the origin, the solution extends to positive values of y for $v_0 > 0$, negative y for $v_0 < 0$. A source distributed along the y-axis gives rise to the concentration field (see e.g., Carslaw and Jaeger, 1959):

$$\chi(y) = \int^y \frac{q(y')}{2sK} \exp\left(-\frac{x^2}{4\kappa(y-y')}\right) \frac{dy'}{y-y'}, \quad (5)$$

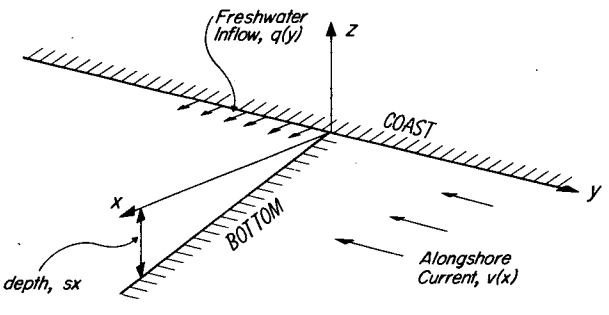

FIG. 1. Inclined plane beach model with freshwater inflow.

where $\kappa = K/v_0$ is a quantity of the physical dimension of length. It is convenient to place the limited line source between $0 < y < Y$ for $v > 0$, and $-Y < y < 0$ for $v < 0$. The freshwater concentration field is then in the two cases:

$$v_0 < 0,\ \kappa < 0 \begin{cases} \chi = \dfrac{q}{2sK} E_1\left(\dfrac{x^2}{4\kappa y}\right), & -Y < y < 0 \\ \chi = \dfrac{q}{2sK}\left[E_1\left(\dfrac{x^2}{4\kappa y}\right) - E_1\left(\dfrac{x^2}{4\kappa(y+Y)}\right)\right], & y < -Y, \end{cases} \quad (6a)$$

$$v_0 > 0,\ \kappa > 0 \begin{cases} \chi = \dfrac{q}{2sK} E_1\left(\dfrac{x^2}{4\kappa y}\right), & 0 < y < Y \\ \chi = \dfrac{q}{2sK}\left[E_1\left(\dfrac{x^2}{4\kappa y}\right) - E_1\left(\dfrac{x^2}{4\kappa(y-Y)}\right)\right], & y > Y, \end{cases} \quad (6b)$$

with (Abramowitz and Stegun, 1964)

$$E_1(z) = \int_z^\infty \frac{e^{-t}}{t}\, dt.$$

The nondimensional density excess will be written

$$\epsilon = \frac{1}{\rho_0}\frac{d\rho}{dS}(S - S_0) \equiv \beta(S - S_0) \quad (7)$$

with S = salinity, S_0 = salinity at zero freshwater concentration, so that

$$\epsilon = -\beta S_0 \chi. \quad (7a)$$

The value of β depends on the T–S relationship applicable to the mixing process between shelf and slope waters. In the Mid-Atlantic Bight in winter this is about $\beta = 0.36$, or $\beta S_0 = 12.6 \times 10^{-3}$.

3. Equation for surface pressure

For the determination of the perturbation pressure field linearized equations of motion may be used because, as mentioned in the introduction, the Rossby number v_0/fL, formed with the *zero-order* advection velocity, is already small. Momentum advection by the zero-order flow is thus negligible, similar advection by the perturbation velocities being of an even smaller order of magnitude. As in previous shelf circulation models, a linear bottom stress law is used, $\tau_b/\rho = rv$. The force of this, distributed over the water column, rvH^{-1}, is typically much larger than the horizontal momentum-flux divergence:

$$K\frac{\partial^2 v}{\partial x^2} = (rvH^{-1}) \approx Ks/rL \ll 1$$

the value of this ratio being 0.1 with the typical quantities used in the calculations. Neglecting thus momentum advection by either zero-order or perturbation flow, and horizontal momentum diffusion, for steady motion and a well mixed water column of depth $H = sx$, the depth integrated equations are

$$\left.\begin{aligned} -\frac{fV}{g} &= -sx\frac{\partial\zeta}{\partial x} - \frac{(sx)^2}{2}\frac{\partial\epsilon}{\partial x} - \frac{\tau_{xb}}{\rho_0 g} \\ \frac{fU}{g} &= -sx\frac{\partial\zeta}{\partial y} - \frac{(sx)^2}{2}\frac{\partial\epsilon}{\partial y} - \frac{\tau_{yb}}{\rho_0 g} \\ \frac{\partial U}{\partial x} &+ \frac{\partial V}{\partial y} = 0 \end{aligned}\right\} \quad (8)$$

with ζ surface elevation and (U, V) the components of transport (depth-integrated velocity). The bottom stress (τ_{xb}, τ_{yb}) will be taken to be proportional to the bottom geostrophic velocity:

$$\left.\begin{aligned} \frac{\tau_{xb}}{\rho_0 g} &= -\frac{r}{f}\frac{\partial\zeta}{\partial y} - \frac{rsx}{f}\frac{\partial\epsilon}{\partial y} \\ \frac{\tau_{yb}}{\rho_0 g} &= \frac{r}{f}\frac{\partial\zeta}{\partial x} + \frac{rsx}{f}\frac{\partial\epsilon}{\partial x} \end{aligned}\right\}, \quad (9)$$

where r is a bottom friction coefficient of the dimension of velocity with a typical magnitude of 5×10^{-4} m s^{-1}.

Substituting the bottom stresses into Eqs. (8) and taking curl, one arrives at the vorticity tendency equation:

$$\nabla_1^2\zeta + \frac{fs}{r}\frac{\partial\zeta}{\partial y} = -sx\nabla_1^2\epsilon - s\frac{\partial\epsilon}{\partial x} - \frac{fs^2x}{r}\frac{\partial\epsilon}{\partial y}. \quad (10)$$

This is very similar in form to the diffusion equation in two dimensions, with the quantity fs/r corresponding to $v_0/K = \kappa^{-1}$, the ratio of an advection velocity (along the y-axis) to horizontal diffusivity. The difference is that fs/r is, in a given hemisphere, always of the same sign, positive north of the equator. Thus the vortex stretching effect of bottom slope produces results akin to advection in the direction of shelf-wave propagation (negative y). Moreover, for a large value of the equivalent advection number,

$$A = \frac{fsY}{r}, \quad (11)$$

where Y is a typical along-isobath scale of the ζ-field, advection along y swamps diffusion in the same way as in the freshwater diffusion problem. The second derivatives of y may then be dropped on both sides of Eq. (10). The simpler equation remains

$$\frac{\partial^2\zeta}{\partial x^2} + \frac{fs}{r}\frac{\partial\zeta}{\partial y} = -sx\frac{\partial^2\epsilon}{\partial x^2} - s\frac{\partial\epsilon}{\partial x} - \frac{fs^2x}{r}\frac{\partial\epsilon}{\partial y}. \quad (12)$$

As is known from similar advection–diffusion problems, the simplification leading to Eq. (12) causes significant errors mainly in the immediate neighbor-

hood of concentrated sources. Other aspects of this approximation were discussed by Csanady (1978), where the heat-conduction analogy was invoked for a physical interpretation of Eq. (12).

Confining attention to coastally trapped pressure fields, the boundary condition at infinity will be taken to be

$$\zeta = 0, \quad x \to \infty. \tag{13}$$

This is consistent with a coastally trapped density field.

At the coast, the depth and the cross-shore transport reduce to zero. So must, by Eqs. (8), the bottom stress, in the absence of wind stress as supposed here. This yields the boundary condition with the aid of Eq. (9):

$$\frac{\partial \zeta}{\partial x} = -sx\frac{\partial \epsilon}{\partial x}, \quad x \to 0. \tag{14}$$

4. Resolution of the pressure field

As suggested by Csanady (1979), it is convenient to split the surface elevation ζ into a generalized dynamic height component ζ_1 and a residual field ζ_2:

$$\zeta = \zeta_1 + \zeta_2,$$

where

$$\frac{\partial \zeta_1}{\partial x} = -\int_{-H}^{0} \frac{\partial \epsilon}{\partial x}\, dz = -sx\frac{\partial \epsilon}{\partial x}. \tag{15}$$

Upon integration, the dynamic height distribution becomes

$$\zeta_1 = -sx\epsilon - s\int_x^\infty \epsilon dx. \tag{16}$$

Because the freshwater plume is long and narrow, this gives an almost two-dimensional pressure distribution, with surface geostrophic velocity nearly parallel to the coast. For a coastally trapped density field, ζ_1 vanishes as $x \to \infty$. By the second of Eqs. (15), the ζ_1-field also satisfies the boundary condition at the coast, so that the conditions on the residual field ζ_2 become

$$\left.\begin{aligned} \frac{\partial \zeta_2}{\partial x} &= 0, \quad x \to 0 \\ \zeta_2 &= 0, \quad x \to \infty \end{aligned}\right\}. \tag{17}$$

Furthermore, backward from all source terms in the time-like y-coordinate ζ_2 is supposed to vanish:

$$\zeta_2 = 0, \quad y \to \infty. \tag{17a}$$

Upon substituting (15) into (12) one finds the differential equation for the residual field

$$\frac{\partial^2 \zeta_2}{\partial x^2} + \frac{fs}{r}\frac{\partial \zeta_2}{\partial y} = \frac{fs^2}{r}\int_x^\infty \frac{\partial \epsilon}{\partial y}\, dx. \tag{18}$$

The only source term in this equation is now due to the cross-isobath baroclinic flow. Interpreted as a vorticity tendency, $\partial\epsilon/\partial y > 0$ tends to produce cyclonic ($\partial\epsilon/\partial y < 0$ anticyclonic) circulation; for further discussion see Shaw and Csanady (1983).

Expressed as hydraulic head, the bottom pressure is

$$\zeta_b = \frac{1}{\rho_0 g} p_b = \zeta + sx\epsilon. \tag{19}$$

Substituting from Eq. (16), this is also

$$\zeta_b = \zeta_2 - s\int_x^\infty \epsilon dx. \tag{20}$$

The components of the bottom geostrophic velocity are

$$\left.\begin{aligned} u_b &= -\frac{g}{f}\frac{\partial \zeta_2}{\partial y} - s\int_x^\infty \frac{\partial \epsilon}{\partial y}\, dx \\ v_b &= \frac{g}{f}\frac{\partial \zeta_2}{\partial x} \end{aligned}\right\}. \tag{21}$$

In the presence of density variations along isobaths, this velocity is divergent, as pointed out by Shaw and Csanady (1983):

$$\frac{\partial u_b}{\partial x} + \frac{\partial v_b}{\partial y} = -\frac{gs}{f}\frac{\partial \epsilon}{\partial y}. \tag{22}$$

In the absence of density variations along isobaths, ζ_2 vanishes everywhere, and so does the bottom geostrophic velocity. Steady flow induced by cross-isobath density gradients alone is then parallel to the isobaths, and is equal to the thermal wind relative to the bottom. The corresponding surface pressure (as hydraulic head ζ_1) is the dynamic height relative to the bottom, and is given by Eq. (16).

With the density field given by Eqs. (6a) or (6b), the ζ_2 equation (Eq. 18, with boundary conditions 17) is readily solved. The right-hand side of (18) represents distributed sources for the ζ_2-field, akin to internal heat generation in the conduction problem, the effects of which are described by the appropriate Green's function.

5. Transport streamlines

The depth-integrated transport is represented by contour lines of the stream function ψ, where

$$V = \frac{\partial \psi}{\partial x}, \quad U = -\frac{\partial \psi}{\partial y}. \tag{23}$$

The replacement of Eq. (10) by (12) is tantamount to the neglect of the x-component bottom stress. Applying the same approximation to Eq. (8) for consistency, one arrives at the expression for ψ:

$$\psi = \frac{g}{f}\int_0^x \left(sx\frac{\partial \zeta_2}{\partial x} - \frac{(sx)^2}{2}\frac{\partial \epsilon}{\partial x}\right)dx$$

$$= \frac{g}{f}\left[sx\zeta_2 - \frac{(sx)^2}{2}\epsilon - s\int_0^x (\zeta_2 - sx\epsilon)dx\right]. \quad (24)$$

This satisfies the coastal constraint, $U = 0$ at $x = 0$, by making the coast a streamline. At large distances from the coast the first two terms in the brackets, proportional to ζ_2 and ϵ, respectively, vanish. The remaining term can be evaluated upon integration of Eq. (18), making use of the boundary conditions (17):

$$\frac{\partial}{\partial y}\int_0^\infty (\zeta_2 - sx\epsilon)dx = 0 \quad (25)$$

or

$$\int_0^\infty \zeta_2 dx = \int_0^\infty sx\epsilon dx + \text{constant}. \quad (25a)$$

The value of the integral on the right follows from the diffusion equation: from Eq. (1), with the y-diffusion term deleted, one finds

$$q(y) = v_0\frac{\partial}{\partial y}\int_0^\infty sx\chi dx = -\frac{v_0}{\beta S_0}\frac{\partial}{\partial y}\int_0^\infty sx\epsilon dx, \quad (26)$$

the second form following from Eq. (7a). Outside the source regions $q(y)$ vanishes, and the integral on the right-hand side of Eq. (25a) becomes constant. The integrated surface level deficiency ζ_2 (equivalent to the total heat content in the conduction analogy) is thus also constant outside the source regions, as is the value of the streamfunction at infinity according to Eq. (24).

In the case of the basic flow toward negative y, both ϵ and ζ_2 vanish at $y > 0$, so that in the same domain both integrals in (25a) are zero, and so is the value of the constant. Hence the streamfunction at infinity vanishes. The entire induced circulation is confined to the half plane $y < 0$. When the zero-order flow is toward positive y, however, one finds at $y > Y$:

$$\int_0^\infty sx\epsilon dx = -\frac{\beta S_0}{v_0}qY = \frac{f}{gs}\psi_\infty, \quad y > Y, \quad v_0 > 0. \quad (27)$$

The backward boundary condition on ζ_2 (Eq. 17a) now shows that the constant in Eq. (25a) is nonzero. At $y < 0$, where ϵ vanishes in this case, one has therefore

$$\int_0^\infty \zeta_2 dx = \frac{\beta S_0}{v_0}qY = \frac{-f}{gs}\psi_\infty, \quad y < 0, \quad v_0 > 0. \quad (28)$$

The streamfunction at infinity thus has a constant value, given by (27) or (28). Physically, one may think of the two integrals in Eqs. (27) and (28) as two independent contributions to the flow field, giving rise to total transport of the same magnitude ψ_∞. In the case of zero-order flow to negative y, the two flow contributions oppose each other in direction, and overlap in space. Thus they cancel each other to some degree, the details depending on just how closely their cross-shore scales coincide. In the case of zero-order flow to positive y, the two flow contributions point in the same direction. They do not, however, overlap so much as replace each other, the transport being handed over from the baroclinic flow of the density field to the barotropic flow of the induced ζ_2-field. This is best seen in the calculated examples below.

With previously used typical parameters, and $q = 100 \times 10^{-4}$ m^2 s^{-1}, $Y = 500$ km, one finds for the total transport of one of the flow components $\beta S_0 q Y v_0^{-1} = 6.3 \times 10^4$ m^3 s^{-1}, or 12.6 times the freshwater inflow rate qY.

6. Calculated examples

For the computations it is convenient to adopt the following scales

$$x, y: \quad l = 4\nu = \frac{4r}{fs},$$

$$\epsilon: \quad \epsilon_0 = \frac{\beta S_0 q}{2sK},$$

$$\zeta: \quad \zeta_0 = \frac{s\epsilon_0 l}{2\gamma},$$

$$\psi: \quad \psi_0 = \frac{gs^2\epsilon_0 l^2}{f},$$

where $\gamma^2 = \nu/|\kappa|$, and $\nu = r/(fs)$, $\kappa = K/v_0$, as used before.

An example with flow toward negative y, which is the forward direction of the parabolic equation (12), is relatively easily calculated. The scaled density field ($\epsilon/\epsilon_0 \rightarrow \epsilon$) is in this case:

$$\epsilon = -E_1\left(-\gamma^2\frac{x^2}{y}\right), \quad -Y < y < 0$$

$$= -E_1\left(-\gamma^2\frac{x^2}{y}\right) + E_1\left(-\gamma^2\frac{x^2}{y+Y}\right), \quad y < -Y, \quad (29)$$

where x, y, Y now stand for x/l, y/l, Y/l. The surface pressure scaled by ζ_0 is

$$\zeta = \zeta_2 + (-4\pi y)^{1/2}\,\text{erfc}\left(\gamma\frac{x}{(-y)^{1/2}}\right), \quad -Y < y < 0$$

$$= \zeta_2 + (-4\pi y)^{1/2}\,\text{erfc}\left(\gamma\frac{x}{(-y)^{1/2}}\right) - [-4\pi(y+Y)]^{1/2}$$

$$\times\,\text{erfc}\left(\gamma\frac{x}{[-(y+Y)]^{1/2}}\right), \quad y < -Y, \quad (30)$$

where ζ_2 is to be calculated as follows:

$$\zeta_2 = \int_{y'=0}^{y} \int_{x'=0}^{\infty} \phi(x', y') \left\{ \exp\left[\frac{(x-x')^2}{y-y'}\right] + \exp\left[\frac{(x+x')^2}{y-y'}\right] \right\} \frac{dx'dy'}{[-(y-y')]^{1/2}} \quad (31)$$

with

$$\phi(x', y') = \frac{1}{(-y')^{1/2}} \operatorname{erfc}\left(\gamma \frac{x'}{(-y')^{1/2}}\right), \quad -Y < y < 0$$

$$= \frac{1}{(-y')^{1/2}} \operatorname{erfc}\left(\gamma \frac{x'}{(-y')^{1/2}}\right) - \frac{1}{[-(y'+Y)]^{1/2}} \times \operatorname{erfc}\left(\gamma \frac{x'}{[-(y'+Y)]^{1/2}}\right), \quad y < -Y.$$

The bottom pressure field is given by

$$\zeta_b = \zeta - 2\gamma x E_1\left(\gamma^2 \frac{x^2}{-y}\right), \quad -Y < y < 0$$

$$= \zeta - 2\gamma x E_1\left(\gamma^2 \frac{x^2}{-y}\right) + 2\gamma x E_1\left(\gamma^2 \frac{x^2}{-(y+Y)}\right), \quad y < -Y. \quad (32)$$

The nondimensional stream function becomes

$$\psi = \frac{1}{2\gamma}\left[x\zeta_2 - \int_0^x \zeta_2(x')dx'\right] + \frac{y}{2\gamma^2}(1 - e^{\gamma^2 x^2/y}), \quad -Y < y < 0$$

$$= \frac{1}{2\gamma}\left[x\zeta_2 - \int_0^x \zeta_2(x')dx'\right] + \frac{Y}{2\gamma^2} + \frac{y}{2\gamma^2} e^{\gamma^2 x^2/y} - \frac{y+Y}{2\gamma^2} e^{\gamma^2 x^2/(y+Y)}, \quad y < -Y. \quad (33)$$

Quantitative parameters used in the calculated examples are shown in Table 1. Figures 2–5 illustrate the calculated fields of density, surface pressure, bottom pressure and transport stream function respectively. The source extends from $y = 0$ to -25 in nondimensional units, or over a 500 km distance, with a total freshwater inflow of 5000 m^3 s^{-1}, about equal to the entire inflow to the Mid-Atlantic Bight over its 1500 km long coastline (Bumpus, 1973).

TABLE 1. Quantitative parameters used in calculations.

Freshwater inflow rate q (m^2 s^{-1})	0.01
Bottom slope s	10^{-3}
Horizontal diffusivity K (m^2 s^{-1})	300
Advection velocity v_0 (m s^{-1})	0.1
Density factor βS_0	12.6×10^{-3}
Friction coefficient r (m s^{-1})	5×10^{-4}
Coriolis parameter f (s^{-1})	10^{-4}
Source length Y (m)	5×10^5
Density deficiency scale ϵ_0	2.1×10^{-4}
Horizontal length scale $l = 4\nu$ (m)	2×10^4
Diffusivity ratio γ	1.291
Surface elevation scale ζ_0 (m)	1.677×10^{-3}
Transport scale ψ_0 (m^3 s^{-1})	8400

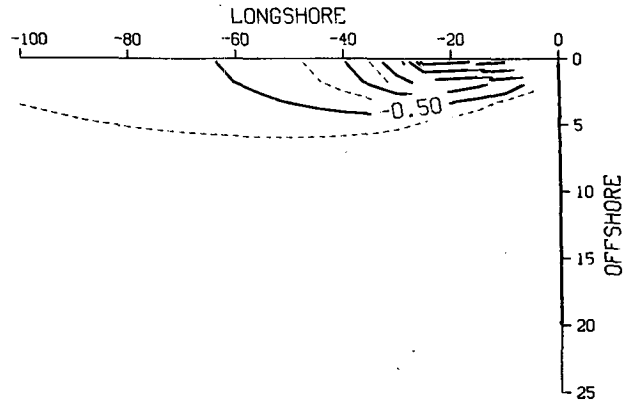

FIG. 2. Contours of constant density, with flow toward negative y and freshening over $-25 < y < 0$. Units of distance are $l = 4\nu = 4r/fs$, of density ϵ_0.

The units of the density in Fig. 2 correspond to 0.21 σ_t-units. The far-field influence is therefore slight, and only close to shore within the source region are density perturbations of order 1 σ_t-unit found. This field is very similar to the one calculated numerically by Shaw (1982). The surface pressure distribution is more or less as expected from the density distribution. The unit here corresponds to 0.163 cm: again, values of order 1 cm are confined to a region close to the source. The bottom pressure distribution is of similar amplitude, but it contains an interesting trough offshore, its deepest point lying just downstream of the source, on the outer shelf (about 80 km from the coast). The function of this trough is to supply fluid for the downstream flow nearshore; see the pattern of transport streamlines. The bottom pressure trough

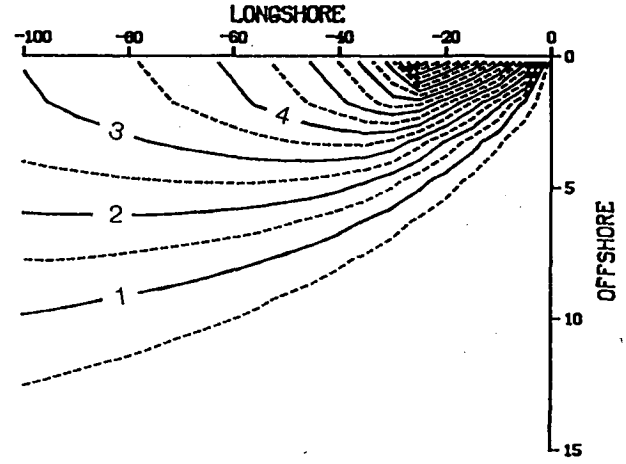

FIG. 3. Distribution of surface pressure, same case as in Fig. 3 (units of ζ_0).

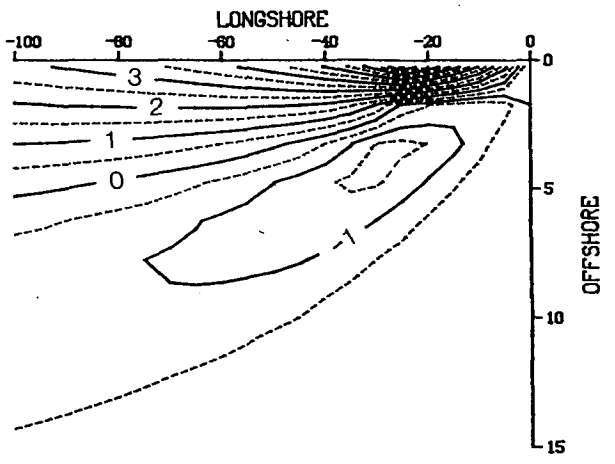

FIG. 4. Distribution of bottom pressure, same case as in Fig. 3 (units of ζ_0). Note low just downstream and offshore from source.

and the associated closed streamline pattern constitutes the crucial difference between the (nearly) two-dimensional view provided by the ζ_1-field and the three-dimensional solution.

The maximum downstream flow induced is about 2.1 in streamfunction units, or 17 600 m^3 s^{-1}, only 3½ times the freshwater inflow rate, or 28% of the maximum calculated from Eq. (28). The reason is that the inflow and outflow regions largely overlap on account of the similarity of scales in the two diffusion equations, (1) and (12) [$\gamma = (\nu/|\kappa|)^{1/2} = 1.29$]. Thus the pressure fields ζ_1 and ζ_2 cancel each other to a considerable extent, leaving only a feeble residual circulation. The character of this circulation follows from the vorticity tendencies associated with the density field, cyclonic where the density increases toward positive y, anticyclonic where the opposite gradient prevails.

The case of advection velocity v_0 opposite to the time-like direction of the parabolic equation (12) (negative y) provides instructive contrast. The density field remains the same by hypothesis (ignoring the distorting effect of perturbation velocities), but the streamlines are quite different (Fig. 6). This case takes much longer computation time, because the whole positive y axis contains source terms for Eq. (12), while the flow is everywhere toward negative y. The pattern shown in Fig. 6 was drawn by hand on the basis of only 27 calculated points, the calculation having taken nearly three hours of computer time. A weak anticyclonic cell near the coast at high positive y does not show up on this coarse grid. Surface and bottom pressure amplitudes are about the same as in the previous case, a bottom pressure trough lying offshore. Because the time-like coordinates of Eqs. (1) and (12) are oppositely directed, there is now no cancellation, and the maximum transport is what one calculates from Eq. (28), 7½ streamfunction units, or 63 000 m^3 s^{-1}.

7. Discussion

The results of the above calculated examples show that, under conditions prevailing in the Mid-Atlantic Bight, the baroclinity–bottom slope interaction makes a weak local contribution to mean circulation, justifying the linearized approach. In the far field, the transports shown in Fig. 5 correspond to maximum velocities less than 0.5 cm s^{-1}, an order of magnitude smaller than the observed long-term mean velocity. They point in the same direction as the long-term mean flow.

Although the details of the flow calculated near the source may not be fully realistic, the cross-isobath transports have to be more or less accurate to satisfy continuity. The values one may read off from Fig. 5 are of order 3×10^{-2} m^2 s^{-1}, corresponding to average cross-isobath velocities of order 0.1 cm s^{-1}. This is much less than cross-isobath flow induced by moderate wind stress.

There are several reasons for the weakness of the induced circulation. One is the cancellation effect mentioned above, brought about by an order-one value of the parameter

$$\gamma^2 = \frac{rv_0}{fsK}.$$

When the flow is opposite to the time-like coordinate of Eq. (12), cancellation does not occur, as seen in Fig. 6. The perturbation velocities are then larger by about a factor of 3 under otherwise identical conditions.

A further contributing factor to small induced transports in the Mid-Atlantic Bight is the smallness of βS_0. This results from the density compensation in the applicable T–S relationship. When cold and fresh water is replaced by warm and saline slopewater, the change in density is rather less than would be due to freshening at constant temperature. The density and pressure fields arising in response to coastal freshening of waters are therefore of lesser amplitude than they would be without the temperature compensation effect, by about a factor of 2½.

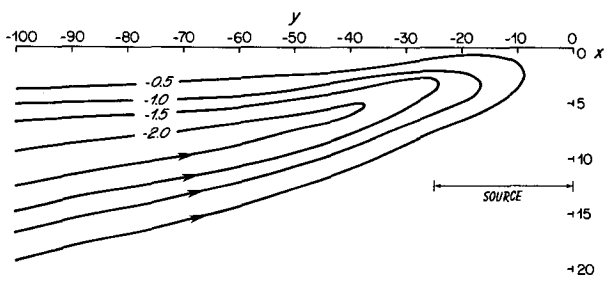

FIG. 5. Streamlines for same case as in Fig. 3 (units of ψ_0). Note that inflow comes from the "forward" time-like direction along the y-axis.

It is interesting to reflect that in the absence of temperature compensation, and without the cancellation effect between the ζ_1 and ζ_2 fields, the calculated perturbation velocities are comparable to the observed mean velocities. Furthermore, on a shelf with weak advection, ψ_∞ becomes high, because the density deficiency increases. Finally, on a steep (e.g., Pacific-type) shelf ψ_∞ is higher because the same density gradients generate larger transports in deeper water, provided of course that the assumptions of the theory are satisfied, i.e., the water column is mixed to the bottom. Thus, while the result of the above investigation shows the freshwater inflow-induced contribution to Mid-Atlantic Bight circulation to be insignificant, it is also clear that this result is site-specific, and that significant large-scale circulation might well arise from land drainage in other locations. Even along the east coast, the weak induced flow into river plumes such as those of the St. Lawrence, Hudson, or the Chesapeake, could be locally important. There is some observational evidence supporting this conclusion (Boicourt, 1982).

The present model also throws further light on the validity of dynamic height calculations in coastal regions. The ζ_1 field gives dynamic heights relative to the bottom (see, for example, the ζ_1 distribution over the east coast shelf shown by Csanady, 1979) and generally suggests a two-dimensional circulation pattern. Geostrophic velocities associated with the ζ_1-field, however, do not give any hint of the inflow or outflow induced by the ζ_2-field, which is necessary to satisfy continuity. On the east coast shelf the main feature of the ζ_1-field is the shelf-edge geostrophic current associated with the front. Given that the front is in some manner a product of upstream freshwater sources, one may legitimately infer considerable cross-isobath transport somewhere in an establishment region of the shelf-edge geostrophic currrent. The two-dimensional view of thermohaline circulation one gains by postulating density contours to be parallel to isobaths (e.g., Csanady, 1978) is presumably a correct zero-order picture, but is certainly incomplete. With the freshwater sources located at the coast, isopycnals must cross isobaths somewhere.

It was pointed out above that the total ζ_2-deficiency is conserved in the wake of a freshwater source [Eq. (28) above]. As discussed elsewhere (Csanady, 1981), the ζ_2-field may be thought of as a cold spot spreading out in the cross-isobath direction, proceeding toward negative y, with the cross-shore scale increasing as $(-ry/fs)^{1/2}$. The slope (dy/dx) of the streamlines is proportional to $(r/fs)^{1/2}$ and becomes small over a steep bottom, or large where f is small. At low latitudes the approximations of the theory break down, but while they remain valid, they suggest steeper streamlines and larger transports (Eq. 28) as f decreases. The one-way transport ψ_∞ for the same qY could thus easily become an order of magnitude greater on a low-latitude shelf than in the Mid-Atlantic Bight, without invalidating the theoretical approach. The corresponding transport, and especially the cross-isobath flow, would then certainly be of practical significance.

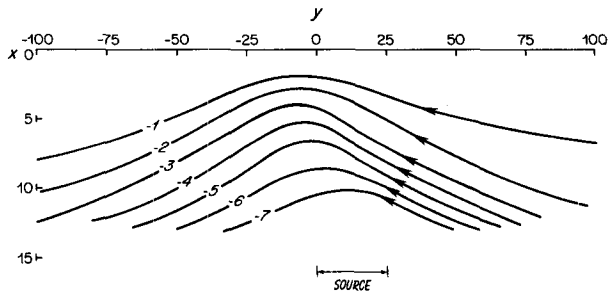

FIG. 6. Streamlines for case of zero-order flow toward positive y. Density field is as in Fig. 3, reflected about the x-axis. The incoming baroclinic (perturbation) flow opposes the zero-order flow and escapes toward negative y. Same units as in Fig. 3.

The case of zero-order advection toward positive y (backward direction of the parabolic equation for ζ) is especially interesting. The freshwater inflow-induced perturbation is in this case inherently more important, as already pointed out, because inflow and outflow do not cancel. The Hudson River plume has occasionally been reported hugging the Long Island shore, instead of the usual New Jersey shore. This is a case corresponding to the illustration of Fig. 6 and should result in more effective offshore transport of river water.

The general principle emphasized by the above results is that geostrophic transports associated with the freshening of coastal waters are subject to continuity. In steady state, closed circulation patterns must arise. Over a sloping shelf, and with bottom friction dominant, streamlines are closed by extending the flow pattern in the forward direction of the parabolic ζ-equation. When other forces dominate, the flow pattern will no doubt be different. It is always a nontrivial question, however, where a baroclinic coastal current comes from and where it goes to.

Acknowledgments. This work was supported by the Department of Energy under a contract entitled "Coastal-shelf transport and diffusion" (Contract No. DE-AC02-79EV10005) and by the Coastal Geography Program of the Office of Naval Research (Contract No. N00014-82-C-0019, NR 083-004). Mr. J. H. Churchill carried out the numerical calculations. I am indebted to a referee for some troubling questions, which led to important clarifications.

REFERENCES

Abramowitz, M., and I. A. Stegun, 1964: *Handbook of Mathematical Functions,* Natl. Bur. Stand., Washington, DC, 1046 pp.

Beardsley, R. C., and C. N. Flagg, 1976: The water structure, mean currents and shelf-water/slope-water front of the New England continental shelf. *Mem. Soc. R. Sci. Liege,* **10,** 209–225.

Blanton, J. O., and L. P. Atkinson, 1983: Transport and fate of river discharge on the Continental Shelf of the Southeastern United States. *J. Geophys. Res.,* **88,** 4730–4738.

Boicourt, W. C., 1982: Estuarine larval retention mechanisms on two scales. *Estuarine Comparisons,* V. S. Kennedy, Ed., Academic Press, 445–457.

Bowman, M. J., and L. D. Wunderlich, 1977: Hydrographic Properties. *MESA New York Bight Atlas Monogr.,* No. 1, New York Sea Grant Inst., Albany, 78 pp.

Bumpus, D. F., 1973: A description of the circulation on the continental shelf of the east coast of the United States. *Progress in Oceanography,* Vol. 6, Pergamon, 111–159.

Carslaw, H. S., and J. C. Jaeger, 1959: *Conduction of Heat in Solids,* 2nd ed. Oxford University Press, 510 pp.

Csanady, G. T., 1978: The arrested topographic wave. *J. Phys. Oceanogr.,* **8,** 47–62.

——, 1979: The pressure field along the western margin of the North Atlantic. *J. Geophys. Res.,* **84,** 4905–4914.

——, 1981: Shelf circulation cells. *Phil. Trans. Roy. Soc. London,* **A302,** 515–530.

——, 1982: *Circulation in the Coastal Ocean, Environ. Fluid Mech. Monogr.,* Reidel, 279 pp.

Hendershott, M., and P. Rizzoli, 1976: The winter circulation of the Adriatic Sea. *Deep-Sea Res.,* **23,** 353–370.

Hsueh, Y., C. Y. Peng and S. L. Blumsack, 1976: A geostrophic computation of currents over a continental shelf. *Mem. Soc. R. Sci. Liege,* **10,** 315–330.

Kao, T. W., 1981: The dynamics of oceanic fronts. Part II: Shelf water structure due to freshwater discharge. *J. Phys. Oceanogr.,* **11,** 1215–1223.

Ketchum, B. H., and D. J. Keen, 1955: The accumulation of river water over the continental shelf between Cape Cod and Chesapeake Bay. *Deep Sea Res.,* **3**(Suppl.), 346–357.

Loder, J. W., D. G. Wright, C. Garrett and B. Joszko, 1982: Horizontal exchange on central Georges Bank. *Can. J. Fish Aquat. Sci.,* **39,** 1130–1137.

Royer, T. C., 1981: Baroclinic transport in the Gulf of Alaska, Part II, Freshwater driven coastal current. *J. Mar. Res.,* **39,** 251–266.

Shaw, P. T., 1982: The dynamics of mean circulation on the continental shelf. Ph.D. dissertation, WHOI-MIT Joint Program in Oceanography and Ocean Engineering, 226 pp.

——, and G. T. Csanady, 1983: Self-advection of density perturbations on a sloping continental shelf. *J. Phys. Oceanogr.,* **13,** 769–782.

Stommel, H., and A. Leetmaa, 1972: Circulation on the continental shelf. *Proc. Nat. Acad. Sci. U.S.A.,* **69,** 3380–3384.